REPORT DOCUMENTATION PAGE

Form Approved OMB NO. 0704-0188

1. REPORT DATE (DD-MM-YYYY)	2. REPORT TYPE	3. DATES COVERED (From - To)
29-07-2013	Final Report	20-Sep-2009 - 19-Mar-2013

4. TITLE AND SUBTITLE
Self Assembly Nonlinear Optical Effects with Novel Small Metal Cluster Systems

5a. CONTRACT NUMBER
W911NF-09-1-0545

5b. GRANT NUMBER

5c. PROGRAM ELEMENT NUMBER
611102

6. AUTHORS
Theodore Goodson III

5d. PROJECT NUMBER

5e. TASK NUMBER

5f. WORK UNIT NUMBER

7. PERFORMING ORGANIZATION NAMES AND ADDRESSES
University of Michigan - Ann Arbor
Regents of the University of Michigan
3003 S. State St
Ann Arbor, MI 48109 -1274

8. PERFORMING ORGANIZATION REPORT NUMBER

9. SPONSORING/MONITORING AGENCY NAME(S) AND ADDRESS(ES)
U.S. Army Research Office
P.O. Box 12211
Research Triangle Park, NC 27709-2211

10. SPONSOR/MONITOR'S ACRONYM(S)
ARO

11. SPONSOR/MONITOR'S REPORT NUMBER(S)
56696-MS.12

12. DISTRIBUTION AVAILIBILITY STATEMENT
Approved for Public Release; Distribution Unlimited

13. SUPPLEMENTARY NOTES
The views, opinions and/or findings contained in this report are those of the author(s) and should not contrued as an official Department of the Army position, policy or decision, unless so designated by other documentation.

14. ABSTRACT
Summary
In the past year, the PI's research on the fundamental properties and applications of nanoclusters has been centered around gold and silver, and many different models have been developed to address the core packing, electron configurations and to explain some of the observed optical properties. Gold and silver in their atomic state shares the same number of valence electrons and bulk packing distance. In this report, we summarize our recent work on

15. SUBJECT TERMS
metal clusters, imaging, surfaces, quantum effects, optical limiting

16. SECURITY CLASSIFICATION OF:			17. LIMITATION OF ABSTRACT	15. NUMBER OF PAGES	19a. NAME OF RESPONSIBLE PERSON
a. REPORT	b. ABSTRACT	c. THIS PAGE			Theodore Goodson III
UU	UU	UU	UU		19b. TELEPHONE NUMBER: 734-647-0274

Report Title

Self Assembly Nonlinear Optical Effects with Novel
Small Metal Cluster Systems

ABSTRACT

Summary
In the past year, the PI's research on the fundamental properties and applications of nanoclusters has been centered around gold and silver, and many different models have been developed to address the core packing, electron configurations and to explain some of the observed optical properties. Gold and silver in their atomic state shares the same number of valence electrons and bulk packing distance. In this report, we summarize our recent work on silver based nanoclusters. Recent work produced stable silver nanoclusters in the condensed phase, purified by gel separation. The basic synthetic approach is similar to that of gold nanoclusters. However, the silver nanoclusters have not been optimized like some other nanoclusters, where high purity can be achieved in a "single-pot" synthesis. Moreover, the stability of silver nanoclusters is also a major concern. By utilizing gel separation methods in their synthesis, our coworkers have been able to purify the nanocluster mixtures to produce highly pure mono-disperse nanoclusters. The result of this work leads to the synthesis of stable silver nanoclusters in high purity, which allows for the identification of silver nanoclusters by mass spectrometry. Due to the very small size of nanocluster and the difficulty in obtaining crystal structures, mass spectrometry has become essential in the identification of nanocluster formula. In this report we focus on the Ag32(SG)19, cluster. The initial interested in silver based system was not solely based on synthetic exploration. One of the most interesting optical property of gold system is its emission and it has tremendous potential in imagining. The larger bandgap of silver (compare to gold) should leads to stronger emission, which would further demonstrate the possibility of using nanoclusters as imaging agents on a cellular level. Ag32(SG)19 also offers an unexplored area in the ultrafast spectroscopy of nanoclusters. This publication aims to report the steady state absorption, the steady state emission spectrum, fluorescence up-conversion and transient absorption of silver nanocluster Ag32(SG)19. The use of ultrafast spectroscopy provides insight into the chemical dynamics of silver nanoclusters. The various optical properties of Ag32(SG)19 provide details regarding the electronic properties of silver clusters, and their possible differences are compared to gold nanoclusters.

Enter List of papers submitted or published that acknowledge ARO support from the start of the project to the date of this printing. List the papers, including journal references, in the following categories:

(a) Papers published in peer-reviewed journals (N/A for none)

Received		Paper
05/23/2013	9.00	Jae Hwan Jung, Joseph C. Furgal, Theodore Goodson, Tomonobu Mizumo, Matthew Schwartz, Kathleen Chou, Jean-François Vonet, Richard M. Laine. 3-D Molecular Mixtures of Catalytically Functionalized [vinylSiO, Chemistry of Materials, (05 2012): 0. doi: 10.1021/cm300587s
05/23/2013	8.00	María Moreno Oliva, Rafael Juárez, Mar Ramos, José L. Segura, Stijn van Cleuvenbergen, Koen Clays, Theodore Goodson, Juan T. López Navarrete, Juan Casado. Linear and Nonlinear Optical Properties of Ramified Hexaazatriphenylenes: Charge Transfer Contributions to the Octupolar Response, The Journal of Physical Chemistry C, (01 2013): 0. doi: 10.1021/jp307563u
05/23/2013	11.00	Sung Hei Yau, Oleg Varnavski, Theodore Goodson. An Ultrafast Look at Au Nanoclusters, Accounts of Chemical Research, (05 2013): 0. doi: 10.1021/ar300280w
05/23/2013	10.00	Sung Hei Yau, Neranga Abeyasinghe, Meghan Orr, Leslie Upton, Oleg Varnavski, James H. Werner, Hsin-Chih Yeh, Jaswinder Sharma, Andrew P. Shreve, Jennifer S. Martinez, Theodore Goodson III. Bright two-photon emission and ultra-fast relaxation dynamics in a DNA-templated nanocluster investigated by ultra-fast spectroscopy, Nanoscale, (2012): 0. doi: 10.1039/c2nr30628j
10/30/2011	2.00	Theodore Goodson, Jeffery E. Raymond. Single-Particle Two-Photon Absorption Imaging and Enhancement Determination for Organic Nanoparticles, The Journal of Physical Chemistry Letters, (02 2011): 0. doi: 10.1021/jz1016558
10/30/2011	3.00	Jeffery E. Raymond, Juan Casado, Juan T. Lopez Navarrete, Kazuo Takimiya, Theodore Goodson. Two-Photon Mediated Three-Photon Fluorescence: Lessons from a Quinoidal Oligothiophene Dimer, The Journal of Physical Chemistry Letters, (09 2011): 0. doi: 10.1021/jz200738t
10/30/2011	4.00	Travis B. Clark, Meghan E. Orr, Daniel C. Flynn, Theodore Goodson. Synthesis and Optical Properties of Two-Photon Absorbing GFP-type Probes, The Journal of Physical Chemistry C, (04 2011): 0. doi: 10.1021/jp2005925
10/30/2011	5.00	Mary Sajini Devadas, Junhyung Kim, Ekkehard Sinn, Dongil Lee, Theodore Goodson, Guda Ramakrishna. Unique Ultrafast Visible Luminescence in Monolayer-Protected Au, The Journal of Physical Chemistry C, (12 2010): 0. doi: 10.1021/jp107033n
10/30/2011	6.00	Michael R. Harpham, Ramakrishna Guda, O?zgu?n Su?zer, Chang-Qi Ma, Peter Ba?uerle, Theodore Goodson, Sergei Tretiak, Ekaterina Badaeva. Excited-State Structure of Oligothiophene Dendrimers: Computational and Experimental Study, The Journal of Physical Chemistry B, (12 2010): 0. doi: 10.1021/jp109624d
10/30/2011	7.00	Theodore Goodson, Guda Ramakrishna, Sung Hei Yau, Oleg Varnavski, John D. Gilbertson, Bert Chandler. Ultrafast Optical Study of Small Gold Monolayer Protected Clusters: A Closer Look at Emission, The Journal of Physical Chemistry C, (09 2010): 0. doi: 10.1021/jp101420g
TOTAL:	**10**	

Number of Papers published in peer-reviewed journals:

(b) Papers published in non-peer-reviewed journals (N/A for none)

Received Paper

TOTAL:

Number of Papers published in non peer-reviewed journals:

(c) Presentations

Number of Presentations: 0.00

Non Peer-Reviewed Conference Proceeding publications (other than abstracts):

Received Paper

TOTAL:

Number of Non Peer-Reviewed Conference Proceeding publications (other than abstracts):

Peer-Reviewed Conference Proceeding publications (other than abstracts):

Received Paper

TOTAL:

Number of Peer-Reviewed Conference Proceeding publications (other than abstracts):

(d) Manuscripts

Received	Paper	
10/30/2011	1.00	Sung Hei Yau, Oleg Varnavski, John D. Gilbertson, Bert Chandler, Guda Ramakrishna, Theodore Goodson III. Au 55 {Ph2P(m-C6H4SO3Na)}12Cl6, a Comparison in the Quantum Size Effect, Journal of Physical Chemistry A (05 2010)

TOTAL: **1**

Number of Manuscripts:

Books

Received	Paper

TOTAL:

Patents Submitted

Patents Awarded

Awards

The Richard Bernstein Distinguished Professor of Chemistry
JILA/NIST Visiting Fellow
AAAS Fellow

Graduate Students

NAME	PERCENT_SUPPORTED
FTE Equivalent:	
Total Number:	

Names of Post Doctorates

NAME	PERCENT_SUPPORTED
FTE Equivalent:	
Total Number:	

Names of Faculty Supported

NAME	PERCENT_SUPPORTED
FTE Equivalent:	
Total Number:	

Names of Under Graduate students supported

NAME	PERCENT_SUPPORTED	Discipline
Brandon Yik	0.50	Chemistry
FTE Equivalent:	**0.50**	
Total Number:	**1**	

Student Metrics

This section only applies to graduating undergraduates supported by this agreement in this reporting period

The number of undergraduates funded by this agreement who graduated during this period:	1.00
The number of undergraduates funded by this agreement who graduated during this period with a degree in science, mathematics, engineering, or technology fields:	1.00
The number of undergraduates funded by your agreement who graduated during this period and will continue to pursue a graduate or Ph.D. degree in science, mathematics, engineering, or technology fields:	1.00
Number of graduating undergraduates who achieved a 3.5 GPA to 4.0 (4.0 max scale):	1.00
Number of graduating undergraduates funded by a DoD funded Center of Excellence grant for Education, Research and Engineering:	0.00
The number of undergraduates funded by your agreement who graduated during this period and intend to work for the Department of Defense	0.00
The number of undergraduates funded by your agreement who graduated during this period and will receive scholarships or fellowships for further studies in science, mathematics, engineering or technology fields:	0.00

Names of Personnel receiving masters degrees

NAME
Total Number:

Names of personnel receiving PHDs

NAME
Sung Hei Yau
Total Number: **1**

Names of other research staff

NAME	PERCENT_SUPPORTED
FTE Equivalent:	
Total Number:	

Sub Contractors (DD882)

Inventions (DD882)

Scientific Progress

This investigation produced stable silver nanoclusters in the condensed phase, purified by gel separation. The basic synthetic approach is similar to that of gold nanoclusters. However, the silver nanoclusters have not been optimized like some other nanoclusters, where high purity can be achieved in a “single-pot” synthesis. Moreover, the stability of silver nanoclusters is also a major concern. By utilizing gel separation methods in their synthesis, our coworkers have been able to purify the nanocluster mixtures to produce highly pure mono-disperse nanoclusters. The result of this work leads to the synthesis of stable silver nanoclusters in high purity, which allows for the identification of silver nanoclusters by mass spectrometry. Due to the very small size of nanocluster and the difficulty in obtaining crystal structures, mass spectrometry has become essential in the identification of nanocluster formula. In this report we focus on the Ag32(SG)19, cluster. The initial interested in silver based system was not solely based on synthetic exploration. One of the most interesting optical property of gold system is its emission and it has tremendous potential in imagining. The larger bandgap of silver (compare to gold) should leads to stronger emission, which would further demonstrate the possibility of using nanoclusters as imaging agents on a cellular level. Ag32(SG)19 also offers an unexplored area in the ultrafast spectroscopy of nanoclusters. This publication aims to report the steady state absorption, the steady state emission spectrum, fluorescence up-conversion and transient absorption of silver nanocluster Ag32(SG)19. The use of ultrafast spectroscopy provides insight into the chemical dynamics of silver nanoclusters. The various optical properties of Ag32(SG)19 provide details regarding the electronic properties of silver clusters, and their possible differences are compared to gold nanoclusters.

Technology Transfer

Self Assembly Nonlinear Optical Effects with Novel Small Metal Cluster Systems

Principal Investigator: ***Theodore Goodson III***
Institution: ***Department of Chemistry, University of Michigan***
Ann Arbor, Michigan 48103
Final Report

Summary

In the past year, the PI's research on the fundamental properties and applications of nanoclusters has been centered around gold and silver, and many different models have been developed to address the core packing, electron configurations and to explain some of the observed optical properties. Gold and silver in their atomic state shares the same number of valence electrons and bulk packing distance. In this report, we summarize our recent work on silver based nanoclusters. Recent work produced stable silver nanoclusters in the condensed phase, purified by gel separation. The basic synthetic approach is similar to that of gold nanoclusters. However, the silver nanoclusters have not been optimized like some other nanoclusters, where high purity can be achieved in a "single-pot" synthesis. Moreover, the stability of silver nanoclusters is also a major concern. By utilizing gel separation methods in their synthesis, our coworkers have been able to purify the nanocluster mixtures to produce highly pure mono-disperse nanoclusters. The result of this work leads to the synthesis of stable silver nanoclusters in high purity, which allows for the identification of silver nanoclusters by mass spectrometry. Due to the very small size of nanocluster and the difficulty in obtaining crystal structures, mass spectrometry has become essential in the identification of nanocluster formula. In this report we focus on the $Ag_{32}(SG)_{19}$, cluster. The initial interested in silver based system was not solely based on synthetic exploration. One of the most interesting optical property of gold system is its emission and it has tremendous potential in imagining. The larger bandgap of silver (compare to gold) should leads to stronger emission, which would further demonstrate the possibility of using nanoclusters as imaging agents on a cellular level. $Ag_{32}(SG)_{19}$ also offers an unexplored area in the ultrafast spectroscopy of nanoclusters. This publication aims to report the steady state absorption, the steady state emission spectrum, fluorescence up-conversion and transient

absorption of silver nanocluster $Ag_{32}(SG)_{19}$. The use of ultrafast spectroscopy provides insight into the chemical dynamics of silver nanoclusters. The various optical properties of $Ag_{32}(SG)_{19}$ provide details regarding the electronic properties of silver clusters, and their possible differences are compared to gold nanoclusters.

A. Steady State Absorption

The steady state absorption spectrum for gold nanoclusters, in particular Au_{25}, has been shown to correlate directly to major transitions calculated from crystal structure.[13,23] For $Ag_{32}(SG)_{19}$ the absorption feature lacks the distinct feature seen for gold systems, instead a major absorption is observed at 500 nm (figure 1). The absorption feature would suggest that Ag_{32} does not have the same packing or metal core arrangement as Au_{25}. However the exact electronic structure of silver nanoclusters has not been calculated due to the lack of crystal structures. The difference is packing of Au_{25} and Ag_{32} can further be support by their mass spectrometry assignment. $Ag_{32}(SG)_{19}$, has a different metal to ligand ratio than $Au_{25}SG_{18}$ and suggests a different metal to ligand bonding motive. The peak at 500 nm of the absorption spectrum also resembles the surface plasmon resonance found for larger nanoparticles. However, direct comparison to the absorption spectrum of Ag nanoparticle (figure 1) shows that the major absorption at 500 nm is 50 nm away of the surface plasmon resonance (SPR). The lack of SPR is a direct evidence of nanocluster formation, an excellent example can be found in pervious publication on gold systems. The lack of SPR also inspires confidence in the similarity between silver and gold nanosystems. Although the metal core packing may be different for silver and gold systems, the lack of SPR suggests that the two systems similar electronically and they are not governed by classical electrostatics. There is another absorption feature at 450 nm, seen as a shoulder (figure 1). These small details in the absorption spectrum has not yet been assigned to specific transitions due to the lack of crystal structures for silver nanoclusters, but supports the idea of nanoclusters as super atoms.[5] The super atom theory uses the gold system as a base model and treats the metal core as a single super atom with distinct electronic transitions, which is vastly different from bulk metal (Mie theory)[39] or nanoparticles. The appearance of fine details in the absorption spectrum is a direct result of the discrete energy level for clusters.[13] The absorption spectrum for Ag nanoclusters would further benefit from smaller clusters core sizes or lower temperature

measurements, both of which would increase the intensity of the fine details in the absorption spectrum, as demonstrated by the ramakrishina group.

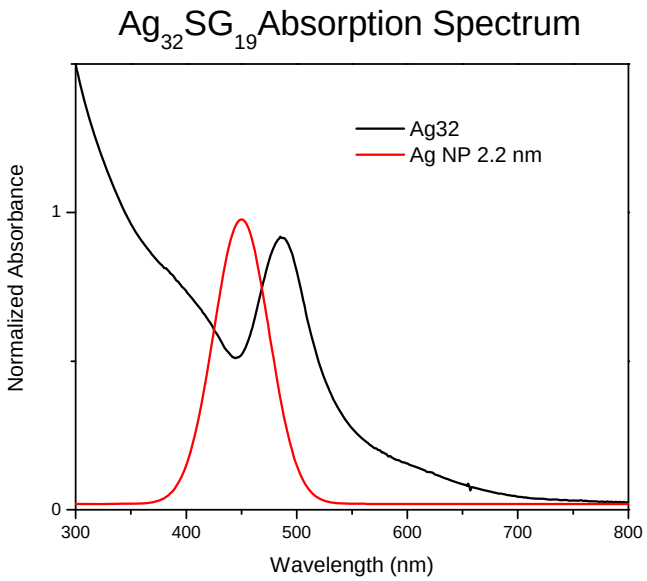

Figure 1: Steady state absorption spectrum for $Ag_{32}(SG)_{19}$ and Ag nanoparticle (2.2 nm). The major absorption peak at 500 nm for the nanocluster is not a SPR respond.

B. Fluorescence

One of the main attractions of silver nanoclusters over gold is the proposed increase in the emission efficiency due to the wider of the homo-lumo gap of silver. For gold nanoclusters, it is well understood that there are two different emissions. One of the emissions originates from the metal core and can be found in the visible region, while a second stronger emission is in the near infrared region. The near infrared emission originates from the ligand-metal surface states. The visible emissions of gold nanoclusters are 5 orders of magnitude stronger than bulk gold, with a quantum yield (Q.Y.) on the order of 1 $x10^{-4}$ [2,36]. $Ag_{32}(SG)_{19}$ exhibits a very strong emission at 650 nm (figure 2) and the maximum emission intensity is measured under 440 nm excitation. The emission wavelength shows no shift under various excitation wavelengths up to 490 nm. A minor shift towards the red is observed at 500 nm. The Q.Y of $Ag_{32}(SG)_{19}$ was

calculated using crystal violet as a standard under various concentration. The Q.Y. of the emission at 650 nm was calculated to be $9x10^{-3}$, almost two orders of magnitude higher than that of gold nanoclusters. The higher Q.Y. suggests that silver is an even better candidate for nanocluster based bio imaging.

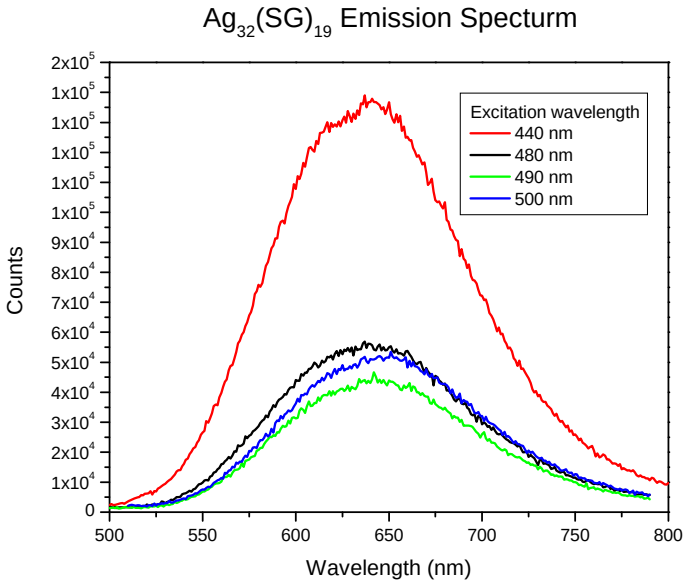

Figure 2: Steady state emission spectra of $Ag_{32}(SG)_{19}$ under various excitation wavelength in the visible region. There are no peak shifts up to 490 nm excitation. A minor shift towards the red can be seen under 500 nm excitation. The maximum emission is observed at 440 nm excitation.

The excitation spectrum has not been widely use in the filed of nanocluster research, but our pervious investigation of DNA-templated silver nanocluster nano-beacon has reveal fine details about the emission process. In the case of $Ag_{32}(SG)_{19}$, it provided extra information that would be otherwise lost in the steady state emission spectrum (figure 3) or the absorption spectrum. The excitation spectrum records the emission intensity as the excitation wavelength changes, and allows for deeper understanding of the major absorptions that contributes to the emission. Using this technique, two different absorption contributes were observed. The two absorption peak directly affects the main emission at 650nm. One of the absorption peaks is at 450 nm while the other peak is at 525 nm (figure 3). The over-lay of the absorption spectrum and

the excitation spectrum reveals that the emission contribution from the main absorption peak at 500 nm does not contribute to the emission directly and suggests that there are energy transfers from the 500 nm to the emissive states. The two absorption features also suggest that the emission may not be simple, which prompt us to investigate further into the emission wavelength.

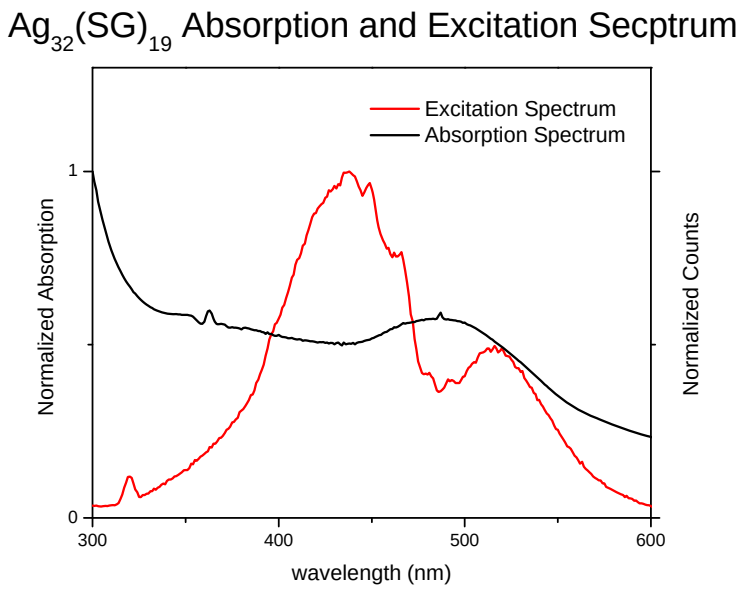

Figure 3: Excitation spectrum for $Ag_{32}(SG)_{19}$ compared to the absorption spectrum. Two separate absorption features can be seen that does not relate to the main absorption peak.

A closer inspection of the emission spectrum reveals that the emission spectrum is non-gaussian in nature, to better resolve the exact emission wavelengths a simple Gaussian model was used. Using a simple sum of the gaussian fits, the emission spectrum can be reproduced with two separate emissions at 609 nm and 664 nm (figure 4). It has been reported that dual emission can be observed for nanoclusters; however, this is the first report of dual emission from nanoclusters both in the visible region. An additional fit centered at 750 nm is used to reproduce the emission spectrum, but it is not considered as a real observable feature due to the uncertainty of wavelength accuracy of the instrument close to 800 nm. Correlating the excitation spectrum and the dual emission wavelengths, the absorption at 450 nm is more closely related to the emission at 609 nm with energy transfer to the 664 nm. The absorption at 525 nm is closely related to 664 nm but does

not couple as strongly to the 609 nm emission, based on the slight wavelength shift under 500 nm excitation seen in figure 2.

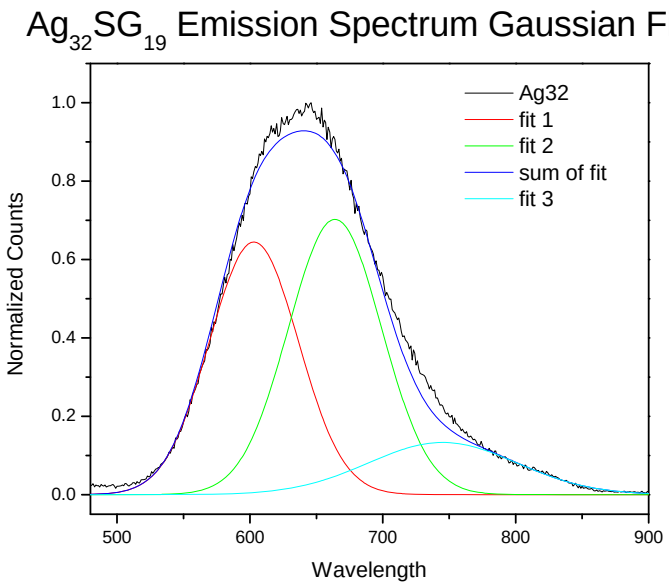

Figure 4: Ag_{32} Emission spectrum fitted using simple Gaussian sums. The peak for fit 1 is at 609 nm and the peak for fit 2 is at 664 nm. Fit 3 is sued to reproduce the spectrum, but is not considered in the final fit due to the wavelength accuracy of the instrument at 800 nm.

C. Mechanism of Emission

To better understand the emission process, fluorescence up-conversion with 60 fs time resolution was used to look at the emission kinetics at 550 nm and 700 nm (figure 5.6, 5.7, 5.8). In theory, if the emission at 650 nm is composed of two different emissions at 609 and 664 nm, the emission processes should be very different, resulting in different kinetics. The fluorescence kinetics at 550 nm shows a life-time of 1.8 ps and 20 ps, (figure 5.6). The kinetics at 700 nm can be fitted with a rise-time of 200 fs, along with two decay times of 400 fs and a very long lived component (figure 5.7). Direct comparison of 550 nm and 700 nm (figure 5.8) should represent the emission at 609 and 664 nm independently (base on our previous gaussian sum in figure 5.5). The emission at 600 nm serves as an intermediate case, closer to the original 650 nm emission (figure 5.8). One of the major differences between the kinetic at 550 nm and 700 nm is the lack of a rise-time component for 500 nm. The lack of a rise-time suggests that the energy

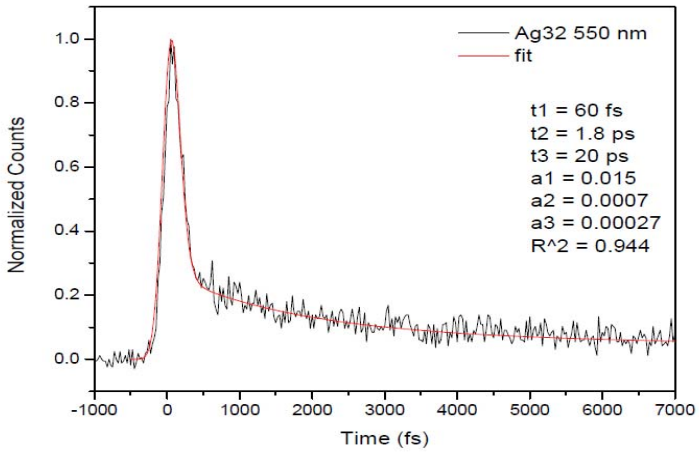

Figure 5 Time resolved visible emission for Ag_{32} at 550 nm.

transfer process is very fast, on the order of the instrument respond (~60fs). This fast energy transfer process correlates closely to the core emission, similar to previously reported life-times for gold nanoclusters.[2] The typical life-times for gold nanoclusters are in the 200 – 300 fs range.[2] The emissions life-time for the 609 nm is 1.8 ps, much longer

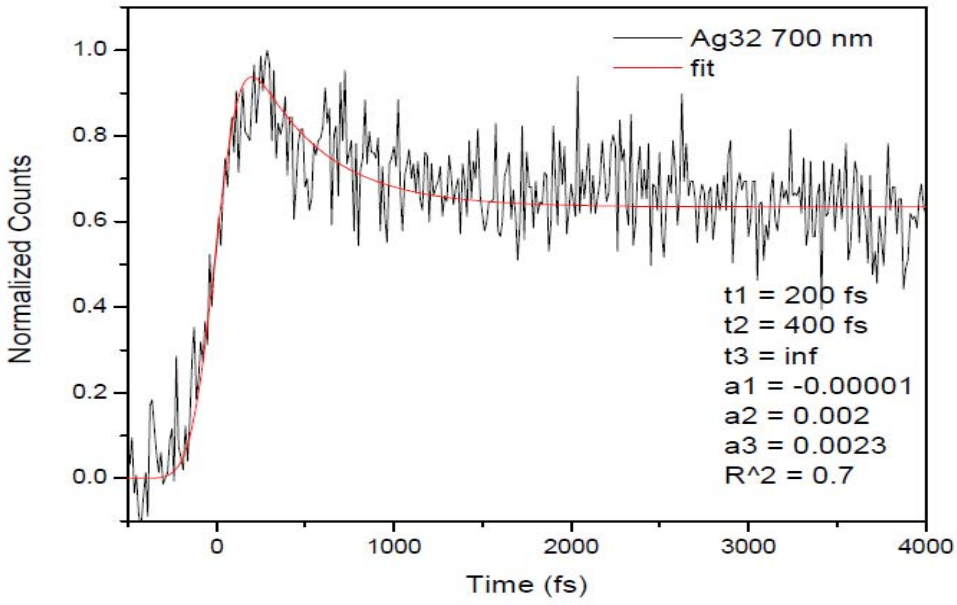

Figure 6 Time resolved visible emission for Ag32 at 700nm.

than gold nanoclusters. The longer life-time can be attributed to the increase in Q.Y and can also be explained by the larger homo-lumo gap of silver in the nanoscale. The emission kinetics at 600 nm is combination of the kinetics at 500 nm and 700 nm and confirms the emission at 650 nm can be separated into 609 nm and 664 nm. For the 664 nm emission, the initial rise-time of 200 fs suggested energy transfer into the emissive state, consistent with our excitation spectrum results. Because energy transfer has to occur before this emission process, we believe that this is similar to the "surface state" proposed for gold systems, where the emission comes from a combined ligand and metal state.[22,35] The ligand itself does not emit.[35] The florescence at 664 nm also has a life time of 400 fs and a very long lived component, the long component is beyond our instrument can measure, and could be longer than 1 ns. Since both emissions have a longer life time than gold nanoclusters, we can further attribute the increase in Q.Y to both increases in the core and surface state emissions.

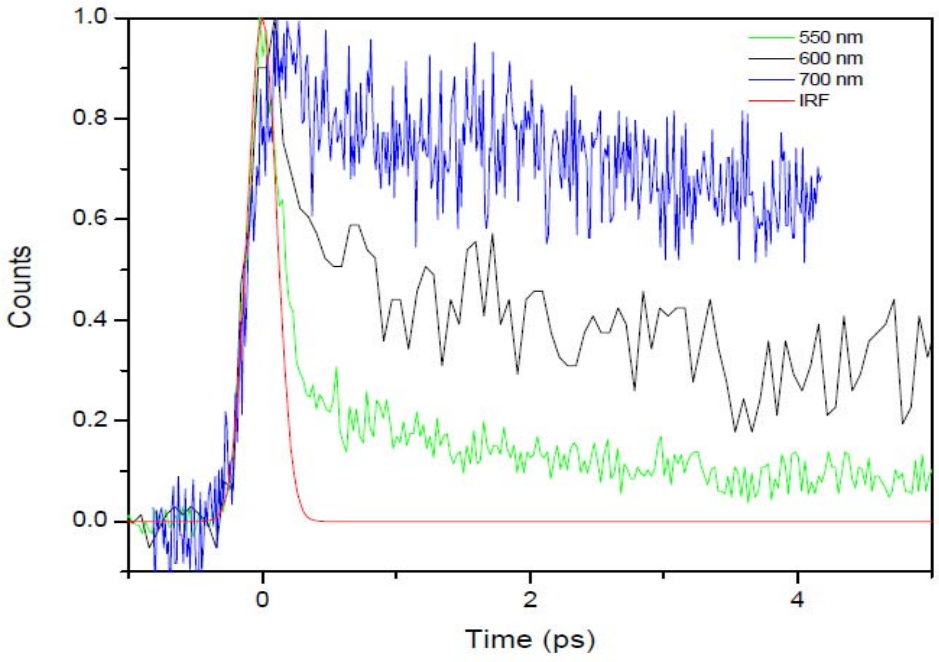

Figure 7 Fluorescence kinetics comparison Ag32.

Looking at the fluorescence kinetics and the steady state spectrum, we proposes a possible emission mechanism for $Ag_{32}(SG)_{19}$ (figure 5.9). The emission mechanism suggests that the two different absorption states at 438 nm and 516 nm contribute to the two emissions at 609 and 664 nm respectively. Under excitation at 400 nm, both emission can be detected and suggests that there are energy transfer between the two absorption states. The emission at 609 nm is fast while the emission at 664 nm is slow. We did not find any experimental result that would indicate and energy transfer between the two emissive states, but there should be some energy transfer between the two absorption states because of the main emission peak at 650 nm is strongest under 440 nm excitation.

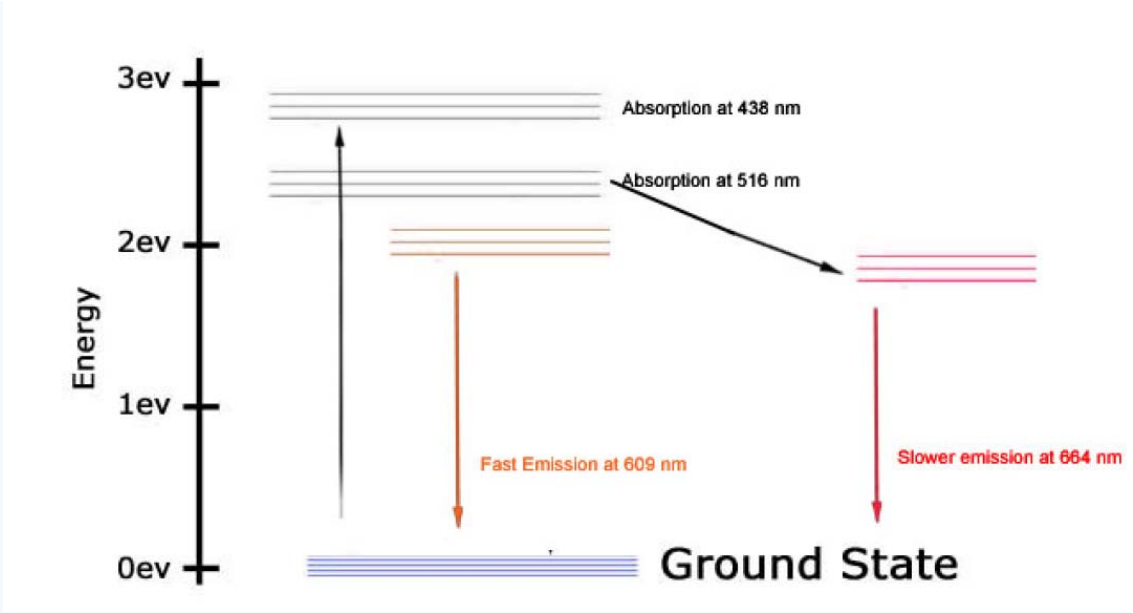

Figure 8: The energy level diagram for silver clusters

Surfaces and Two-Photon NSOM Studies

In the last year we have been successful in our studies of putting the metal clusters on surfaces to investigate their optical properties and applications in the solid state. The student working on this is Nerengha Abeyasinghe and part of this work has been submitted to *Nature Photonics* for publication. New approaches in molecular nanoscopy are still needed for interrogation of biological, organic, and inorganic objects

with sizes in the diffraction-unlimited realm. There have been advances in diffraction-limited imaging techniques to obtain transverse *point resolutions* on the order of ~30 nm. With the application of tip-enhanced near-field scanning optical microscopy (NSOM) ~20 nm point resolution has been obtained. Multi-photon (TPEF) fluorescence NSOM is able to also realize an enhanced point resolution attributive of NSOM due to its independence of diffraction and strong intensity dependence. However, previous reports of TPEF NSOM using an aperture based NSOM could not improve point resolutions beyond 175 nm (>λ/5). Also, rapid photo-damage of typical TPEF chromophores under high TPEF excitation intensities limits the success of this approach. However, with the use of quantum-confined Au_{25} monolayer protected nanoclusters (NCs) as robust two photon absorbers we report the first observation of TPEF NSOM with a ***point resolution*** of ~36 nm **(<λ/22)**. Additionally, the calculated two photon absorption cross section (δ_{solid}) value for Au_{25} NCs in solid state is **1,320,000 GM**, which is greatly enhanced compared to the solution phase result. It was found that the absence of a solvent nano-environment in the case of a solid substrate causes exciton-phonon coupling effects to be reduced, increasing the oscillator strength of the specific transition. With their excellent photo-stability, Au_{25} NCs emit strong TPEF giving rise to a ***point resolution*** that was previously unattainable with aperture-based TPEF NSOM. *This* contribution opens a new avenue toward imaging nanometer-sized objects utilizing TPEF NSOM with quantum confined gold NCs which is a very promising direction for super-resolution imaging, high density data storage, and ultrasensitive sensing.

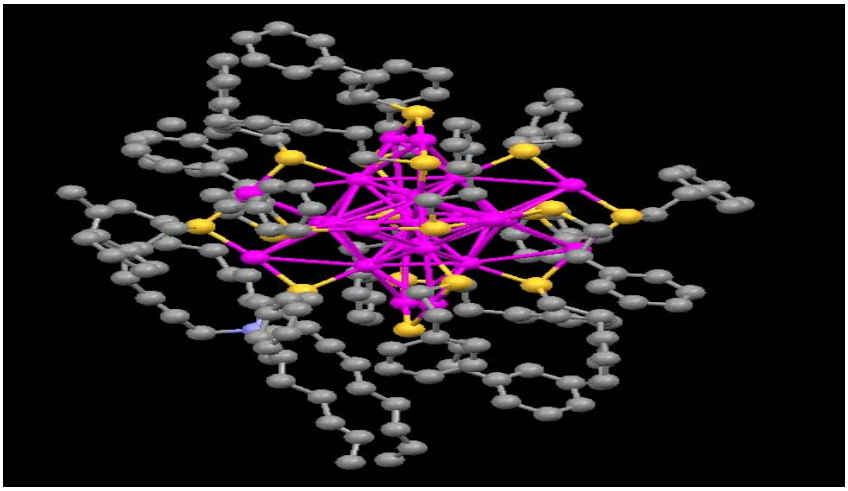

Figure 9: The crystal structure of Au25 with ligands attached.

Our measurements included AFM image spanning a 1 µm x 1 µm field of view of a glass cover slip possessing single NC concentrations (surface density D_s < *11 molecules/* μm^2). The features circled in green in figure 6 are a result of tip convoluted AFM images of single NCs. The vertical scale bar corresponds to AFM thickness in nm after background subtraction. (b) TPEF NSOM image (after background noise subtraction) of $Au_{25}(PET)_{18}$ single nanoclusters (surface density D_s < *6 molecules/* μm^2) using 810 nm femtosecond excitation pulses spanning a 1 µm x 1 µm field of view. The vertical scale bar is in counts/200 ms. The features circled in blue are TPEF NSOM of single nanocluster emitters. Scans were performed using 4 nm pixel sizes at 20 ms bin times. (c) 810 nm femtosecond output from the Mai Tai is sent through a system of optics and coupled to a single mode optical fiber. (M1 through M6 are reflective mirrors, I1: iris, C1 and C2: collimating lenses, NDF: neutral density filter, FOC: fiber optic coupler, SMOF: Single mode optical fiber) (d), the near-filed illumination geometry inside the NSOM is depicted. The excitation is done in the near-field (<<<λ) using the illumination mode excitation with collection of the transmitted and fluorescence photons in the far-field using an inverted objective.

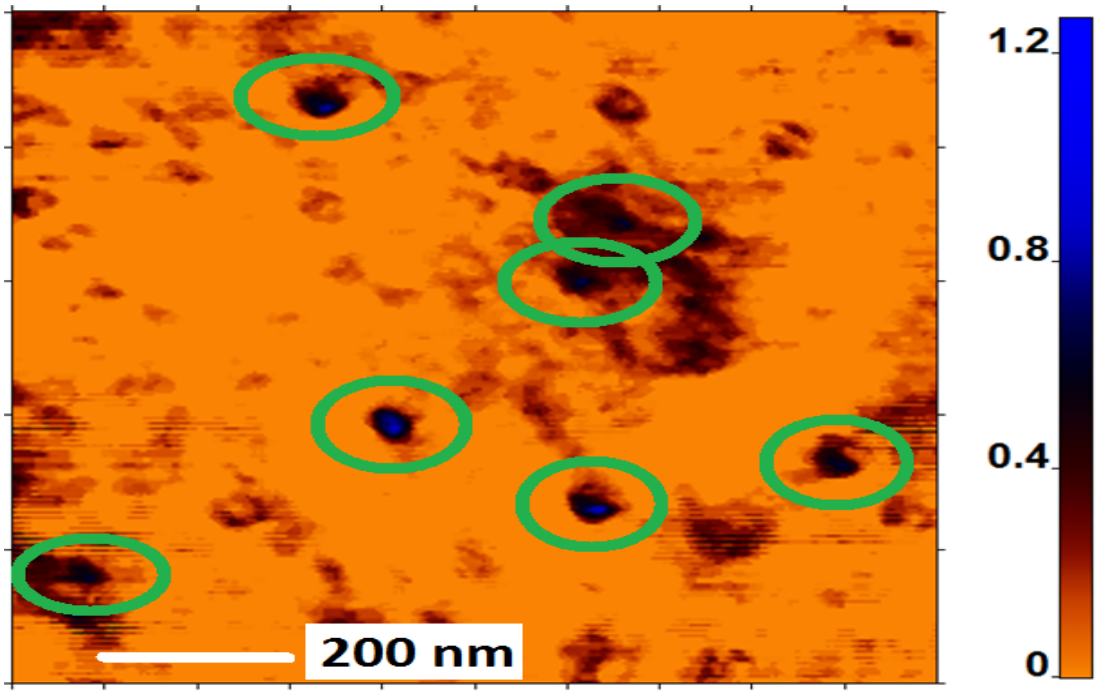

Figure 10: The AFM images of Au25.

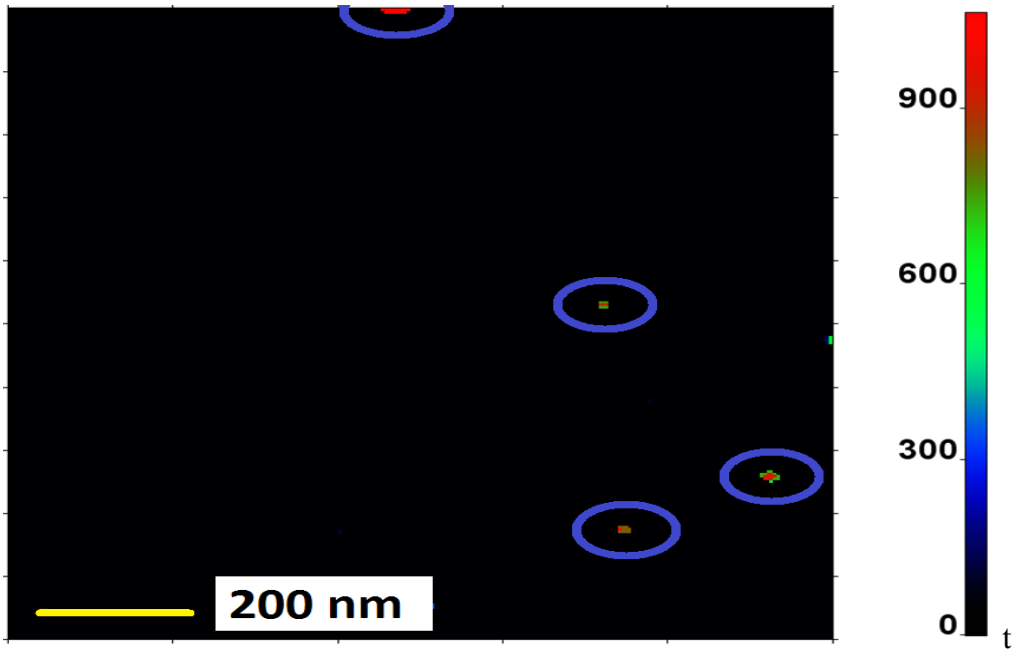

)

in chemistry.

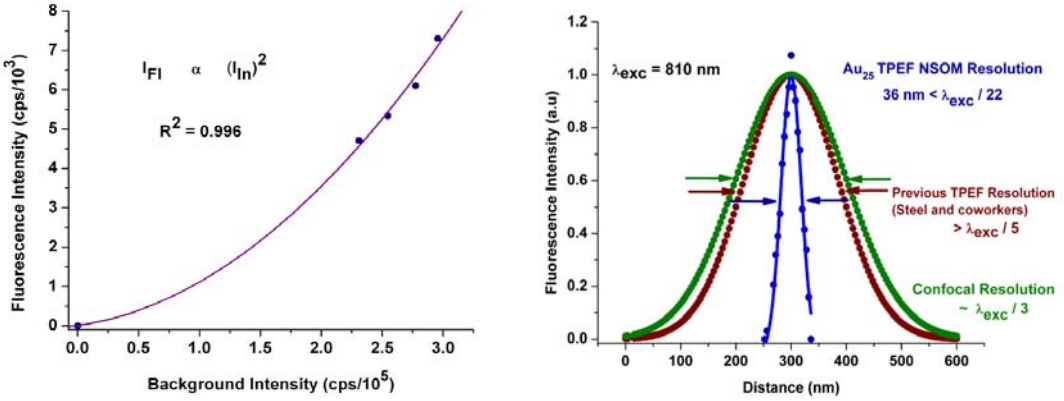

Figure 11 Au25 gold clusters ,t he left panel is the AFM image and the right panel is the two photon NSOM image. These are the first such images ever taken.

(a) Plot of quadratic dependence of fluorescence intensity on incident intensity with 810 nm excitation. The intensity-squared dependence is an indication of the presence of TPEF NSOM. Horizontal axis – background intensity (cps/10^5), Vertical axis – maximum

fluorescence intensity (cps/10^3) of single cluster NSOM image of a single feature. (b) Transverse point resolution attainable with confocal fluorescence microscopy (green) is ~ 200 nm (~$\lambda/3$) [13] whereas the resolution obtained by Steel and coworkers using TPEF NSOM of Rhodamine B dye molecules produced a FWHM of 175 nm (>$\lambda/5$) [11]. Conversely, the point resolution **36±2 nm (<λ/22)** FWHM for TPEF NSOM of $Au_{25}(PET)_{18}$ single nanocluster emitters (blue) in the current work evidently surpasses the previously observed value. Gaussian plots for the confocal resolution and previous TPEF NSOM resolution were simulated to depict appropriate FWHM resolution. The data in blue color are taken directly from the averaged line scan data and fitted for a Gaussian function.

IV. Reference:

(1) Jin, R. *Nanoscale* **2010**, *2*, 343–62.

(2) Yau, S. H.; Varnavski, O.; Goodson, T. *Accounts of chemical research* **2013**.

(3) Parker, J. F.; Fields-Zinna, C. A.; Murray, R. W. *Accounts of chemical research* **2010**, *43*, 1289–96.

(4) Sun, D.; Gong, X.; Wang, X.-Q. *Physical Review B* **2001**, *63*, 193412.

(5) Walter, M.; Akola, J.; Lopez-Acevedo, O.; Jadzinsky, P. D.; Calero, G.; Ackerson, C. J.; Whetten, R. L.; Grönbeck, H.; Häkkinen, H. *Proceedings of the National Academy of Sciences of the United States of America* **2008**, *105*, 9157–62.

(6) Negishi, Y.; Nobusada, K.; Tsukuda, T. *Journal of the American Chemical Society* **2005**, *127*, 5261–70.

(7) Negishi, Y.; Takasugi, Y.; Sato, S.; Yao, H.; Kimura, K.; Tsukuda, T. *Journal of the American Chemical Society* **2004**, *126*, 6518–9.

(8) Devadas, M. S.; Bairu, S.; Qian, H.; Sinn, E.; Jin, R.; Ramakrishna, G. *The Journal of Physical Chemistry Letters* **2011**, *2*, 2752–2758.

(9) Ramakrishna, G.; Varnavski, O.; Kim, J.; Lee, D.; Goodson, T. *Journal of the American Chemical Society* **2008**, *130*, 5032–3.

(10) Varnavski, O.; Ramakrishna, G.; Kim, J.; Lee, D.; Goodson, T. *Journal of the American Chemical Society* **2010**, *132*, 16–7.

(11) Hicks, J. F.; Miles, D. T.; Murray, R. W. *Journal of the American Chemical Society* **2002**, *124*, 13322–13328.

(12) Jadzinsky, P. D.; Calero, G.; Ackerson, C. J.; Bushnell, D. A.; Kornberg, R. D. *Science (New York, N.Y.)* **2007**, *318*, 430–3.

(13) Zhu, M.; Aikens, C. M.; Hollander, F. J.; Schatz, G. C.; Jin, R. *Journal of the American Chemical Society* **2008**, *130*, 5883–5.

(14) Negishi, Y.; Chaki, N. K.; Shichibu, Y.; Whetten, R. L.; Tsukuda, T. *Journal of the American Chemical Society* **2007**, *129*, 11322–3.

(15) Akola, J.; Walter, M.; Whetten, R. L.; Häkkinen, H.; Grönbeck, H. *Journal of the American Chemical Society* **2008**, *130*, 3756–7.

(16) Schmid, G. *Chemical Society reviews* **2008**, *37*, 1909–30.

(17) Templeton, A. C.; Wuelfing, W. P.; Murray, R. W. *Accounts of Chemical Research* **2000**, *33*, 27–36.

(18) Varnavski, O.; Goodson, T.; Mohamed, M.; El-Sayed, M. *Physical Review B* **2005**, *72*, 235405–.

(19) Miller, S. A.; Womick, J. M.; Parker, J. F.; Murray, R. W.; Moran, A. M. *The Journal of Physical Chemistry C* **2009**, *113*, 9440–9444.

(20) Varnavski, O.; Ispasoiu, R. G.; Balogh, L.; Tomalia, D.; Goodson, T. *The Journal of Chemical Physics* **2001**, *114*, 1962.

(21) Qian, H.; Y. Sfeir, M.; Jin, R. *The Journal of Physical Chemistry C* **2010**, *114*, 19935–19940.

(22) Devadas, M. S.; Kim, J.; Sinn, E.; Lee, D.; Goodson, T.; Ramakrishna, G. *The Journal of Physical Chemistry C* **2010**, *114*, 22417–22423.

(23) Aikens, C. M. *The Journal of Physical Chemistry C* **2008**, *112*, 19797–19800.

(24) Desireddy, A.; Kumar, S.; Guo, J.; Bolan, M. D.; Griffith, W. P.; Bigioni, T. P. *Nanoscale* **2013**, *5*, 2036–44.

(25) Kumar, S.; Bolan, M. D.; Bigioni, T. P. *Journal of the American Chemical Society* **2010**, *132*, 13141–3.

(26) Guo, J.; Kumar, S.; Bolan, M.; Desireddy, A.; Bigioni, T. P.; Griffith, W. P. *Analytical chemistry* **2012**, *84*, 5304–8.

(27) Wu, Z.; Suhan, J.; Jin, R. *Journal of Materials Chemistry* **2009**, *19*, 622.

(28) Shichibu, Y.; Negishi, Y.; Tsukuda, T.; Teranishi, T. *Journal of the American Chemical Society* **2005**, *127*, 13464–5.

(29) Heaven, M. W.; Dass, A.; White, P. S.; Holt, K. M.; Murray, R. W. *Journal of the American Chemical Society* **2008**, *130*, 3754–5.

(30) Briant, C. E.; Theobald, B. R. C.; White, J. W.; Bell, L. K.; Mingos, D. M. P.; Welch, A. J. *Journal of the Chemical Society, Chemical Communications* **1981**, 201.

(31) Wang, G.; Guo, R.; Kalyuzhny, G.; Choi, J.-P.; Murray, R. W. *The journal of physical chemistry. B* **2006**, *110*, 20282–9.

(32) Lin, C.-A. J.; Lee, C.-H.; Hsieh, J.-T.; Wang, H.-H.; Li, J. K.; Shen, J.-L.; Chan, W.-H.; Yeh, H.-I.; Chang, W. H. *Journal of Medical and Biological Engineering* **2009**, *29*, 276–283.

(33) Shibu, E. S.; Muhammed, M. A. H.; Tsukuda, T.; Pradeep, T. *Journal of Physical Chemistry C* **2008**, *112*, 12168–12176.

(34) Chevrier, D. M. *Journal of Nanophotonics* **2012**, *6*, 064504.

(35) Dreaden, E. C.; El-Sayed, M. A. *Accounts of chemical research* **2012**, *45*, 1854–65.

(36) Yau, S. H.; Varnavski, O.; Gilbertson, J. D.; Chandler, B.; Ramakrishna, G.; Goodson, T. *The Journal of Physical Chemistry C* **2010**, *114*, 15979–15985.

(37) Yau, S. H.; Abeyasinghe, N.; Orr, M.; Upton, L.; Varnavski, O.; Werner, J. H.; Yeh, H.-C.; Sharma, J.; Shreve, A. P.; Martinez, J. S.; Goodson, T. *Nanoscale* **2012**, *4*, 4247–54.

(38) Plech, A.; Cerna, R.; Kotaidis, V.; Hudert, F.; Bartels, A.; Dekorsy, T. *Nano letters* **2007**, *7*, 1026–31.

(39) Mie, G. *Annalen der Physik* **1908**, *330*, 377–445.

(40) Kubo, R.; Kawabata, A.; Kobayashi, S. *Annual Review of Materials …* **1984**, 49–66.

(41) Wang, G.; Huang, T.; Murray, R. W.; Menard, L.; Nuzzo, R. G. *Journal of the American Chemical Society* **2005**, *127*, 812–3.

1.